

Galvanomagnetic properties of AsF₅-intercalated graphite

W. LANG, A. PHILIPP, K. SEEGER

Ludwig Boltzmann Institut für Festkörperphysik, Kopernikusgasse 15, A-1060 Wien, Austria and Institut für Festkörperphysik der Universität Wien, Strudlhofg. 4, A-1090 Wien, Austria

The galvanomagnetic properties of AsF₅-intercalated, highly-oriented, pyrolytic graphite (HOPG) were determined for stages 1 to 4 in the temperature range from 4.2 to 300 K using contactless eddy current methods for the measurement of electrical conductivity and magnetoresistance and a new inductive technique for the Hall effect. From the results p-type conduction, mean carrier mobility, total carrier concentration and charge transfer are deduced. The mobility is diminished upon intercalation due to an effective mass increase when the Fermi level is shifted by charge transfer from AsF₅ to graphite layers. Charge transfer reaches a maximum of $\frac{1}{3}$ for stage-2 compounds. The temperature dependence of galvanomagnetic effects yields carrier scattering at crystallite boundaries for low temperatures and scattering at phonons of both intercalated layers and graphite sheets for higher temperatures. Magnetoresistance of low-stage compounds exhibits anomalies at low temperatures resulting in an overestimation of mobility and saturation at magnetic field strengths where the low field approximation still should be valid. For magnetic fields of several kiloGauss a reduction of the magnetoresistance was observed. It is suggested that these effects are due to trigonal warping of the graphite energy bands and to diffuse scattering at crystallite boundaries.

1. Introduction

Graphite is an anisotropic semimetal whose properties can be altered by intercalating with dopants which may be either of electron donor (e.g. alkali metals) or acceptor type (e.g. Lewis acids like AsF₅) between the carbon layers. The intercalant layers are periodically arranged between the graphite sheets, with the number of continuous graphite layers between adjacent intercalated layers denoting the stage index n , leading to the stoichiometric formula C _{n} AsF₅ for graphite/arsenic pentafluoride intercalation compounds. Charge transfer from intercalant to graphite layers results in an enhancement of the carrier density in the carbon sheets and evokes metal-like electronic properties such as a plasma edge in the optical reflectivity and high electrical conductivity [1, 2].

The graphite intercalation compounds (GICs) with arsenic pentafluoride have especially aroused great interest because of their high electrical conductivity parallel to the carbon sheets (σ_{ab}) of about half the value of copper at room temperature [3, 4]. These compounds also exhibit an extremely high electrical anisotropy, being quasi two-dimensional conductors with ratio σ_{ab}/σ_c , where σ_c is the conductivity in the direction perpendicular to the graphite planes, greater than 10^6 [2]. The anisotropy of AsF₅-GICs restricts conventional measuring methods for a determination of transport properties. It is impossible to achieve homogeneous current distribution in AsF₅ intercalated samples by conventional point contacts.

Therefore eddy current methods were developed for the measurement of electrical conductivity and mag-

netoresistance [5]. Several attempts to determine the main parameter of interest, the charge transfer f , defined as the ratio of free carrier concentration to intercalant molecule concentration were made by conductivity and magnetoresistance [5], optical reflectivity [1], Pauli spin susceptibility [6], and quantum oscillation measurements [7-9]. A new eddy current technique for the measurement of the Hall effect in highly anisotropic conductors permits the determination of the carrier concentration in the temperature range from 4.2 to 300 K. Electrical conductivity, magnetoresistance and Hall effect of graphite/AsF₅ intercalated to the stages $n = 1$ to $n = 4$, were determined on the very same sample as a function of temperature.

2. Experimental techniques

2.1. Sample preparation

AsF₅-GICs were synthesized from highly-oriented pyrolytic graphite (HOPG), grade ZYH, which was delivered by Union Carbide. The spread of the c -axes in this polycrystalline material is $3.5^\circ \pm 1.5^\circ$. The surface of the samples exhibits a slight texture in contrast to samples with better c -axes alignment. Samples were cut by sand blasting with 40 μ m SiC powder to the desired disk-shape, necessary for the eddy current methods for galvanomagnetic measurements described below. Thickness was reduced by cleaving with a razor blade. A hole for a wire in the centre of the graphite disk to be used as a probe was drilled with a conventional twist-drill since structural defects in this region of the sample are not crucial. HOPG samples were of 0.6 to 1.0 cm diameter and

0.09 to 0.17 cm thick. Before intercalation, the samples were heated to 800°C for at least 5 h under a dynamic vacuum of 5×10^{-6} torr to remove adsorbed water vapour. The heating process yields a weight loss of 2%. Without this treatment no intercalation was observed for a period of several days. Afterwards the sample was introduced into the intercalation apparatus and stored under vacuum.

The apparatus consists of a "Pyrex" reactor with a screw cap with teflon gasket and a stainless steel and teflon valve system which allows direct exposure of the graphite sample to AsF_5 vapour with pressure of 1 bar at room temperature. The intercalation process was controlled by monitoring the sample thickness with a microscope with calibrated reticule. Plateaux in the sample thickness–time function, related to the complete and uniform intercalation of a particular stage as reported by Falardeau *et al.* [10], were observed. This "staging" effect permits a well-defined termination of the intercalation process near the end of a plateau corresponding to the desired stage. Since AsF_5 -GICs are not stable in vacuum, excess AsF_5 had to be removed by rinsing the reactor with argon. Only samples with good correlation of thickness increase and AsF_5 -weight uptake with theoretical values deduced from covalent atomic radii and the stoichiometric formula C_nAsF_5 of AsF_5 -GICs were used for galvanomagnetic measurements to ensure well-characterized, homogenous compounds. It was also possible to synthesize well-defined stage 4 compounds in contrast to Falardeau *et al.* [10], which may be a consequence of the lower AsF_5 pressure (~ 0.8 bar) during our reaction.

Although the intercalation process is similar for all samples, some differences occur in the first intercalation step towards a stage 5 compound which varies from 5 to 30 min. This may be due to microcracks perpendicular to the stacking direction. Hooley [11] pointed out that the intercalation process begins at the two surface layers of a cylindrical sample. In the case of microcracks, the number of surface layers is increased and the process starts at different parts of the sample, resulting in a higher reaction speed.

After intercalation with AsF_5 the samples were transferred into a glove box with argon atmosphere and contacted with 70 μm diameter gold wire and gold paint. Since stage 1 and 2 compounds lost approximately 4% of weight per day at room temperature even in an inert environment, the AsF_5 -GICs were encapsulated in "Pyrex" ampoules and stored in liquid nitrogen. In this way, the total weight loss until the end of the measurement could be limited to below 1%, preventing sample changes between the characterization of the samples and the galvanomagnetic investigations.

2.2. Conductivity and magnetoresistance measurements

The electrical conductivity of a sample was determined by measuring the change in mutual inductance of a pair of coaxial coils upon introduction of the graphite/ AsF_5 compound due to induced eddy currents. The axis of the disk-shaped sample was oriented

parallel to the axes of the coils to ensure current flow only in the highly conducting two-dimensional graphite planes. A second pair of adjustable coils connected in reverse polarity was used to zero the signal with empty measuring coils. A lock-in amplifier was used to select the phase of the signal related to the conductivity of the sample. A small change of the nulling signal with temperature was recorded and used as an offset value for the measurements. The mutual inductance change due to the ohmic eddy current losses in the sample is related to the electrical conductivity according to a theory by Rorschach and Herlin [12]. The agreement between experimental results and theory was tested with metal samples of known conductivity and found to be excellent in the non-skin depth limited regime. To prevent a skin effect in highly conducting AsF_5 -intercalated HOPG samples, an excitation frequency of 400 Hz was chosen. This method needs no extensive calibration procedure like data evaluation by a semi-empirical theory [13] and avoids erroneous measurements possibly occurring at high (e.g. 100 kHz) frequencies [2].

Since eddy current methods are very sensitive to conducting materials outside the measuring coil system, standard cryogenic techniques with metal cryostats are not applicable. Temperatures from 4.2 to 77 K were achieved by passing a steady flow of cold helium gas through the sample holder in a glass cryostat with a liquid nitrogen heat shield. Temperature control was performed by a thermocouple near the sample and a heater in the gas inlet pipe. For temperatures between 77 and 300 K the sample holder was heated with warm helium gas above the ambient temperature of the surrounding liquid nitrogen heat shield.

For magnetoresistance measurements, an additional d.c. magnetic field B_0 , generated by an electromagnet, is applied parallel to the sample axis. The circular current path in the graphite disk remains unchanged when applying B_0 as a consequence of a radial Hall voltage which will be discussed in the next section. Transverse magnetoresistance is calculated from the change of the in-plane electrical conductivity measured by the mutual inductance method while sweeping B_0 in either polarity with a frequency of 3 mHz. Magnetic field control and data acquisition was performed by a computer. At high temperatures, where the magnetoresistance is low, the sweep was repeated several times, taking the mean value of the measurements to improve the signal-to-noise ratio. A calibrated Hall probe was used to measure the magnetic field. The distance of the pole pieces of the electromagnet was 8 cm to provide space for the cryostat tail and to minimize the influence on the measuring coils. The maximum magnetic field obtainable was 10 kG.

2.3. Measurement of the Hall mobility

The conventional four-probe Hall effect method with filamentary samples is not successful for AsF_5 -intercalation compounds for two reasons [7]: it is not possible to achieve a well-defined current distribution in the sample by point contacts due to the extremely high anisotropy of acceptor compounds [13]. On the

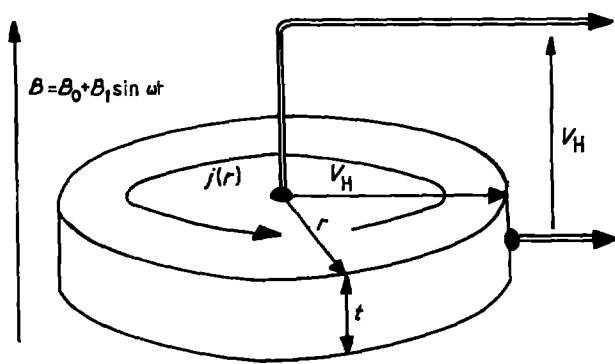


Figure 1 Disk-shaped sample of radius r and thickness t for galvanomagnetic measurements. For Hall mobility determination, two contacts at the centre and at the circumference of the sample are needed.

other hand, charge transfer from the intercalant to the graphite layers results in a high carrier density which leads to a very small Hall voltage in the classical arrangement. For these reasons, previous results on alkali-metal GICs of much lower anisotropy are contradictory even concerning the sign of the Hall effect [14]. In order to overcome this restriction to Hall effect measurements, a new eddy current technique was developed, based on the same disk-shaped sample geometry as the mutual inductance method. So it is possible to determine electrical conductivity, magnetoresistance, and Hall effect on the very same sample, a fact very important considering the structural variations between various HOPG pieces.

For a description of the method see Fig. 1. Circular eddy currents with a current density $j(r)$, depending on the central distance r , are induced by a small alternating magnetic field B_1 with angular frequency ω . If an additional strong, static magnetic field B_0 parallel to B_1 and to the sample axis is applied, the charged carriers are subject to the Lorentz force and deflected from the circular path to a spiral motion. In the described geometry the Lorentz force, oriented in the direction perpendicular to both $j(r)$ and B_0 , acts radially. Like in the classical arrangement, the resulting Hall voltage, V_H , counteracts exactly the Lorentz force to establish unchanged current paths. V_H is probed by two contacts at the centre and at the circumference of the sample, which have no influence on the current distribution if the input impedance of the lock-in amplifier, used for the detection of V_H , is high enough (100 M Ω) to minimize the current flow.

Assuming, that the excitation frequency of the eddy current, ω is low enough to prevent a skin effect, the relative permeability of the sample equals 1 and, neglecting magnetoresistance, the Hall voltage V_H is given by:

$$V_H = \mu_H (r/2)^2 B dB/dt \quad (1)$$

where μ_H is the Hall mobility which is the product of the Hall factor r_H being of the order of 1 and the drift mobility. B is the total magnetic field consisting of the static magnetic field B_0 and the field B_1 exciting the eddy current:

$$B = B_0 + B_1 \sin \omega t \quad (2)$$

Consequently, the Hall voltage at the input of the lock-in amplifier is:

$$V_H = \mu_H \omega (r/2)^2 (B_0 B_1 \cos \omega t + B_1^2 \sin 2\omega t) \quad (3)$$

Since the lock-in amplifier is synchronized to ω and $B_0 \gg B_1$, the second term in brackets is negligibly small. The sign of the Hall coefficient R_H was determined via the relation $\mu_H = R_H \sigma_{ab}$ from the phase shift of V_H relative to the exciting field B_1 . Hole conduction yields the same phase as a p-doped silicon reference sample. For negatively charged carriers, an additional phase shift of 180° was observed according to the negative sign of R_H . Thermovoltages, thermomagnetic effects, geometric and induction voltages are cancelled by sweeping B_0 to both polarities and taking mean values. It is noteworthy, that the thickness, t , of the sample does not enter Equation 3, an indication for the compatibility of the method with two-dimensional conduction. Also it is seen from Equation 1 that the Hall voltage, V_H , is proportional to the mobility, a parameter rather large in GICs, and not to the inverse carrier concentration, which would lead to an extremely small Hall effect in the classical configuration.

A more detailed description of these eddy current techniques for galvanomagnetic measurements will be published elsewhere [15].

3. Results

The galvanomagnetic properties of graphite/AsF₅ samples of stages 1 to 4 were investigated in the temperature range from 4.2 to 300 K.

The room temperature conductivities of AsF₅-GICs of stages 1 to 4 compared with the results of other authors are given in Table I. A maximum room temperature conductivity of about half the value for copper was achieved for stage 2 compounds. Conductivity values for all stages are somewhat lower than previous results [2–4], which may be due to the greater mosaic spread in the starting material. The conductivity ratio $\sigma_{ab}(4.2\text{ K})/\sigma_{ab}(300\text{ K})$ of grade ZYH HOPG, generally used as a quality parameter, was only between 2 and 3, although the room temperature conductivity was $2.3 \times 10^4 (\Omega\text{ cm})^{-1}$, the same value as in high-grade material [16].

Using the sheet conductor model proposed by Spain and Nagel [17] and Dresselhaus and Leung [18], the electrical conductivity of the highly conducting graphite layers, neighbouring the intercalant gallery, was determined to be $5.2 \times 10^5 (\Omega\text{ cm})^{-1}$ from a fit to the conductivity–stage data.

The electrical conductivity of graphite/AsF₅ is plotted in Fig. 2 for temperatures ranging from 4.2 to

TABLE I Room temperature conductivities, in units of $10^5 (\Omega\text{ cm})^{-1}$, of graphite/AsF₅ intercalation compounds of different stages in comparison with published results

Reference	Stage			
	$n = 1$	$n = 2$	$n = 3$	$n = 4$
Present work	2.0–2.8	2.4–3.0	1.9–2.8	1.8–2.1
Interrante <i>et al.</i> [3]	3.0	3.2	2.8	1.9
Thompson <i>et al.</i> [4]	3.0–3.1	2.9–3.2	3.0–3.1	2.4
Foley <i>et al.</i> [2]	3.7–5.0	5.3–6.3	5.0–5.9	–

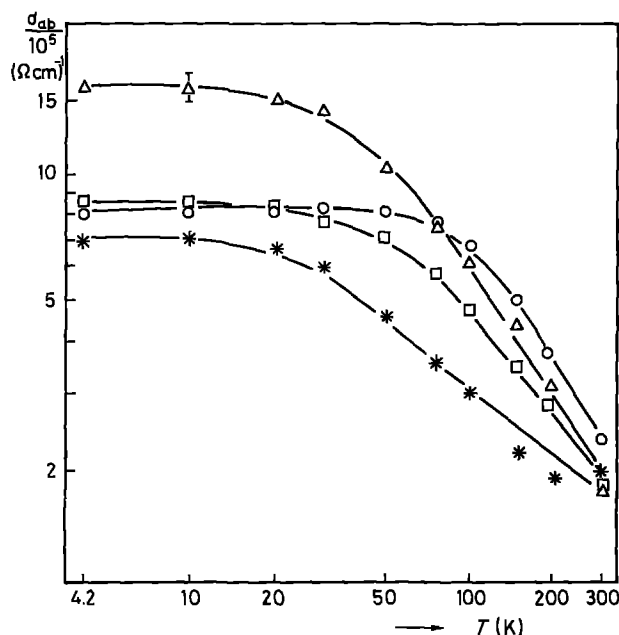


Figure 2 Electrical in-plane conductivity, σ_{ab} , of graphite/AsF₅ compounds (C₃₆AsF₅) plotted against temperature T for intercalation stage 1 (*), stage 2 (○), stage 3 (△) and stage 4 (□). Error-bar is representative of all data points.

300 K. A metal-like behaviour was observed for all samples. The temperature dependence of the electrical conductivity follows a T^{-1} law for stages 2 to 4 above 100 K and saturates to a residual resistivity below 20 to 50 K, depending on stage. All samples exhibit a similar temperature dependence of the electrical conductivity. The degradation from the T^{-1} law of stage 1 GIC may be due to structural imperfections and was not observed on all stage 1 samples. A more detailed analysis in the temperature range from 77 to 300 K, carried out on another set of samples, is shown in Fig. 3, where the electrical conductivity is plotted against the inverse temperature. For stage 1 and 2 GICs a linear dependence is seen with changes in slope at 140 and 130 K, respectively. This indication of an

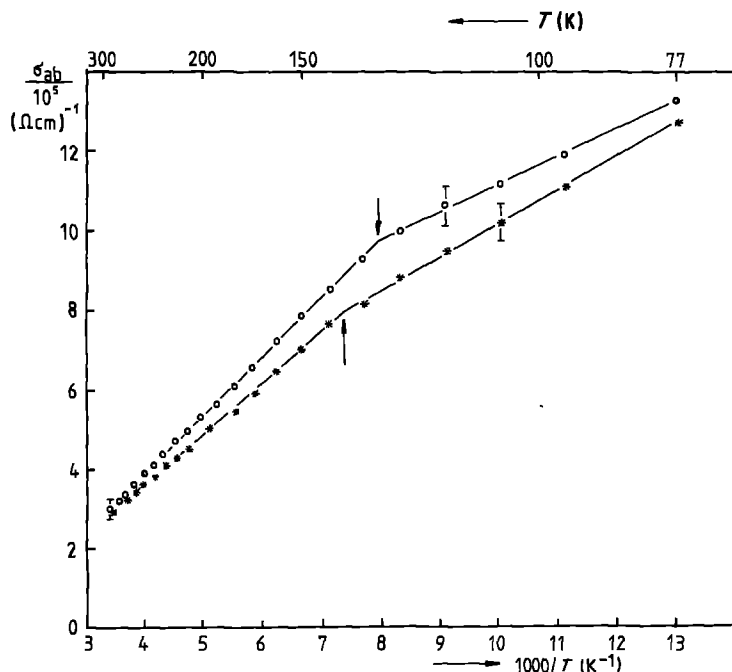


Figure 3 Electrical in-plane conductivity σ_{ab} of graphite/AsF₅ compounds (C₃₆AsF₅) of stage 1 (*) and stage 2 (○) plotted against the inverse temperature T^{-1} . Electronic phase transition temperatures at 140 K (stage 1) and 130 K (stage 2) are indicated by arrows.

electronic transformation has been interpreted as an onset of ordering of the intercalated AsF₅ molecules towards lower temperatures [5]. NMR results [19] and conduction electron spin resonance [20], however, indicate a more gradual ordering between ~ 140 and ~ 220 K. In stages 3 and 4 no kink in the temperature dependence of the electrical conductivity was observed, which may be related to a less perfect intercalation structure with small admixtures of adjacent stages.

Transverse magnetoresistance $\Delta\rho/\rho_0$ was investigated in magnetic fields up to 10 kG for stage 1 to 4 samples at temperatures between 4.2 and 300 K. Fig. 4 shows a plot of $\Delta\rho/\rho_0$ against B^2 at room temperature. Quadratic magnetoresistance according to a simple one-band conduction model

$$\Delta\rho/\rho_0 = (\mu_M B)^2 \quad (4)$$

was found for all samples and for low values of B , where $\mu_M B \ll 1$ is valid. μ_M is the magnetoresistance mobility, related to the drift mobility μ by $\mu_M = \mu T_M$, T_M being the magnetoresistance scattering factor which is of the order of 1. From the slopes of the curves, the magnetoresistance mobilities were determined, yielding a continuous decrease from high-stage to low-stage compounds.

In Fig. 5, $\Delta\rho/\rho_0$ is plotted against B^2 at 77 K. The magnetoresistance is proportional to B^2 only for very small magnetic fields. For samples of stages 3 and 4, quadratic behaviour changes to linear above 2 kG; for the low-stage compounds $n = 1$ and $n = 2$, the magnetoresistance saturates at 3.5% and 4.5%, respectively, at magnetic fields greater than 6 kG. Using the quadratic regime of magnetoresistance for the evaluation of μ_H , again a decrease with enhanced intercalation was observed. This behaviour of the magnetoresistance cannot be explained in terms of a single carrier model.

In Fig. 6 $\Delta\rho/\rho_0$ is plotted as a function of B at 4.2 K. The magnetoresistance is quadratic only for magnetic

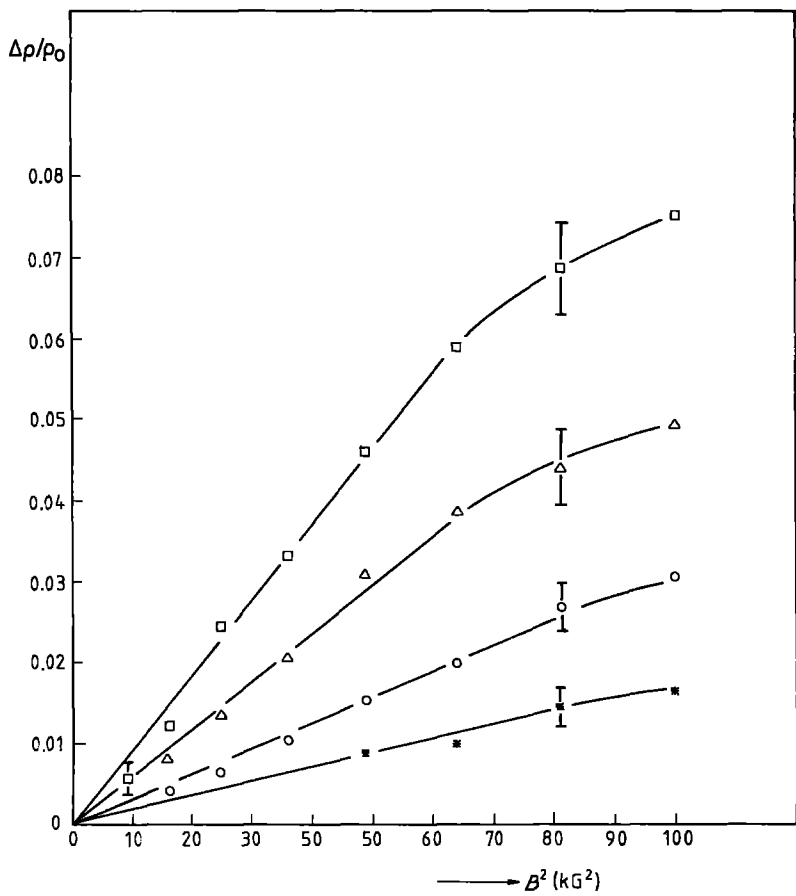


Figure 4 Transverse magnetoresistance $\Delta\rho/\rho_0$ of graphite/ AsF_5 compounds ($\text{C}_{6n}\text{AsF}_5$) plotted against the square of the magnetic field B^2 for stage 1 (*), stage 2 (O), stage 3 (Δ), and stage 4 (\square) at 300 K.

fields of several hundred Gauss. In a stage 4 sample, $\Delta\rho/\rho$ changes to a linear relationship in B above 2 kG and reaches a value of 1 at 10 kG. Up to this magnetic field strength, no saturation occurs. The magnetoresistance of the stage 3 sample exhibits a flat peak at 4 kG and slightly decreases towards higher magnetic fields. This behaviour is even more enhanced in the stage 1

AsF_5 -GIC. $\Delta\rho/\rho_0$ reaches 8% at 3.5 kG and then continuously decreases to about zero at 10 kG. Negative magnetoresistance was not observed, but from the slope of the curve near 10 kG it seems reasonable to expect $\Delta\rho/\rho_0 < 0$ for magnetic fields greater than 10 kG. The stage 2 sample exhibits qualitatively the same behaviour as $n = 1$ with a higher peak value of

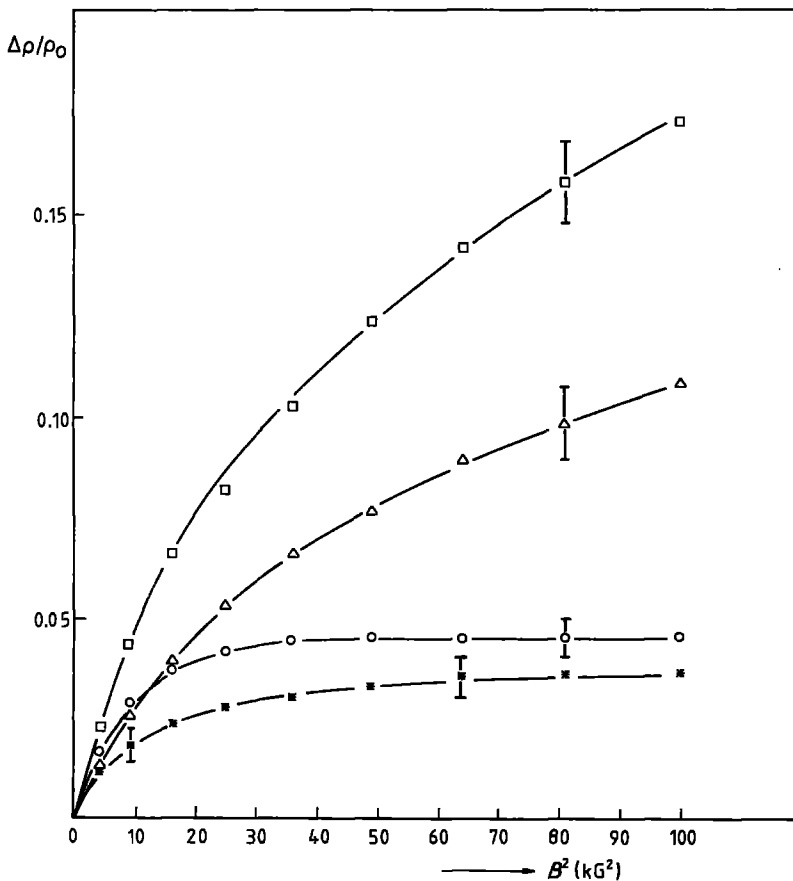


Figure 5 Transverse magnetoresistance $\Delta\rho/\rho_0$ of graphite/ AsF_5 compounds ($\text{C}_{6n}\text{AsF}_5$) plotted against the square of the magnetic field B^2 for stage 1 (*), stage 2 (O), stage 3 (Δ) and stage 4 (\square) at 77 K.

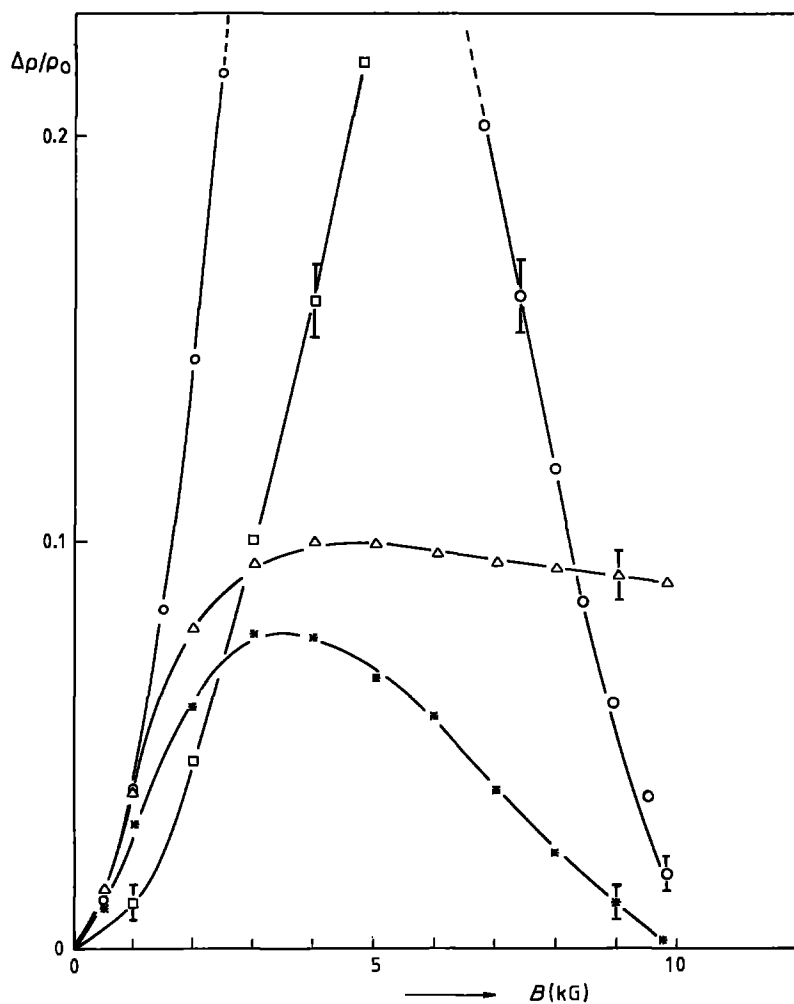


Figure 6 Transverse magnetoresistance $\Delta\rho/\rho_0$ of graphite/AsF₅ compounds (C_{8n}AsF₅) plotted against the magnetic field B for stage 1 (*), stage 2 (○), stage 3 (Δ) and stage 4 (□) at 4.2 K.

$\Delta\rho/\rho_0$. The observed anomaly of the magnetoresistance is limited to temperatures below 30 K. In Fig. 7, $\Delta\rho/\rho_0$ of the stage 1 sample is plotted against B for various temperatures between 4.2 and 30 K. It is clearly seen, that the magnetoresistance decrease above 4 kG is washed out with raising temperature. In the low-field regime, no difference in magnetoresistance for temperatures up to 30 K was observed.

The Hall-effect of AsF₅-GICs was measured for the first time, employing the eddy current method described above, in the temperature range 4.2 to 300 K on the same set of samples as used for conductivity and magnetoresistance measurements. The sign of the Hall coefficient, R_H , was positive for all stages, which intimates that the carriers are predominantly holes. This carrier type is consistent with the chemistry of the intercalation reaction proposed by Bartlett *et al.* [21]. The AsF₅ molecules disproportionate by electron uptake from the graphite lattice according to



The Hall voltages rose slightly sublinear with increasing B , which is due to a reduction of eddy current intensity caused by magnetoresistance. After correction by applying the corresponding $\Delta\rho/\rho_0$ values, a strictly linear relationship between V_H and B was observed. Hence the Hall coefficient R_H is independent of B and a mean Hall mobility can be deduced from the Hall voltage according to Equation 3. μ_H is plotted as a function of temperature in Fig. 8. The behaviour

of μ_H is quite similar for all stages. Two regions can be distinguished. Between 100 and 300 K μ_H decreases with temperature following a potential law: $\mu_H \propto T^{-0.7}$. Below 50 K the Hall mobility tends asymptotically to a constant low-temperature value. The two regimes are associated with phonon scattering and scattering of the carriers at crystallite boundaries, respectively.

The mobility of graphite is decreased upon intercalation with AsF₅. For stage 3 samples, μ_H equals the values of stage 4. Room temperature mobility is diminished after intercalation to stage 1 to one decade below the initial value of HOPG. At first sight this seems to be due to defect generation by the intercalation process. Hence from Fig. 8 it is seen that phonon scattering predominates at 300 K, leaving the mobility reduction mainly due to an effective mass increase from $0.039m_0$ (HOPG) to $0.38m_0$ (C₈AsF₅) [7, 22] caused by a shift of the Fermi level away from the band edge upon intercalation. The total hole concentration p was calculated from the values of electrical conductivity and Hall mobility, assuming for simplicity a single-band model and taking $r_H = 1$:

$$p = \frac{\sigma_{ab} r_H}{e \mu_H} \quad (6)$$

Results are plotted in Fig. 9 for temperatures from 4.2 to 300 K. With the exception of a flat increase towards low temperatures for the stage 3 sample, no temperature dependence of the hole concentration was

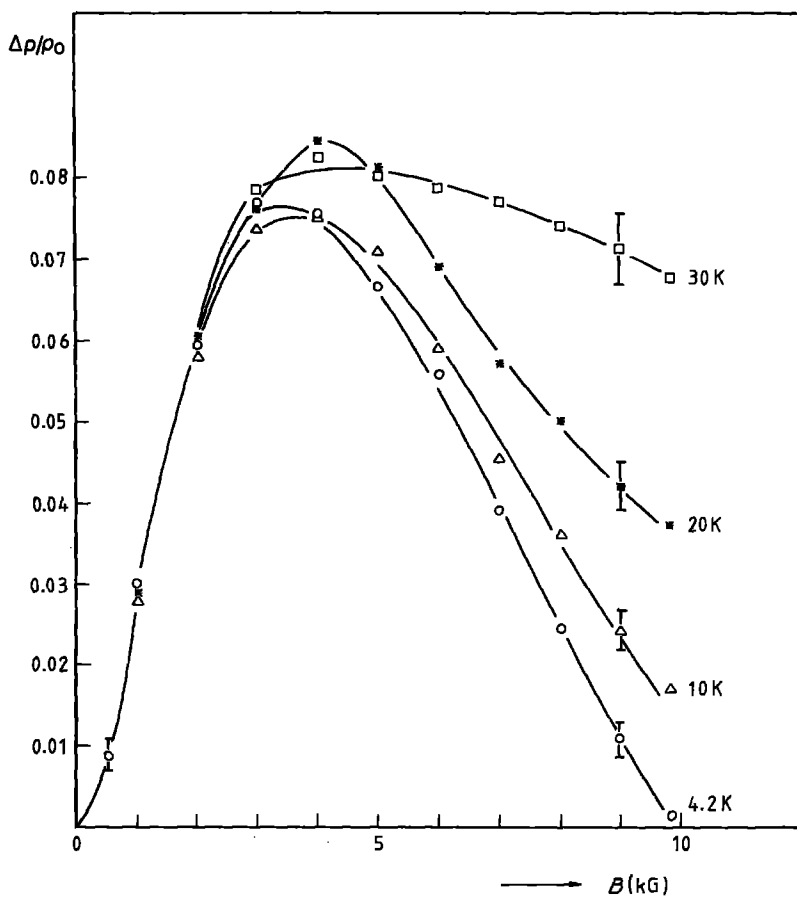


Figure 7 Transverse magnetoresistance $\Delta\rho/\rho_0$ of a stage 1 graphite/ AsF_5 compound ($\text{C}_{8n}\text{AsF}_5$) plotted against magnetic field B for various temperatures between 4.2 and 30 K.

observed. This supports the opinion that p is determined by charge transfer from the intercalant layers only and described by the disproportioning reaction Equation 5. Previous results by Zeller *et al.* [5], indicating a decrease of p below 50 K are falsified by an overestimation of the mobility, which was determined from magnetoresistance, due to an anomaly to be discussed later. Carrier concentration increases upon intercalation up to $1.6 \times 10^{21} \text{ cm}^{-3}$ for stage 1 and 2

compounds, being two orders of magnitude greater than in HOPG and two orders lower than in conventional metals.

4. Discussion

As a general tendency it was observed that the influence of structural imperfections in the starting HOPG is reduced upon intercalation with AsF_5 . For example Zeller *et al.* [5] used HOPG with a conductivity ratio

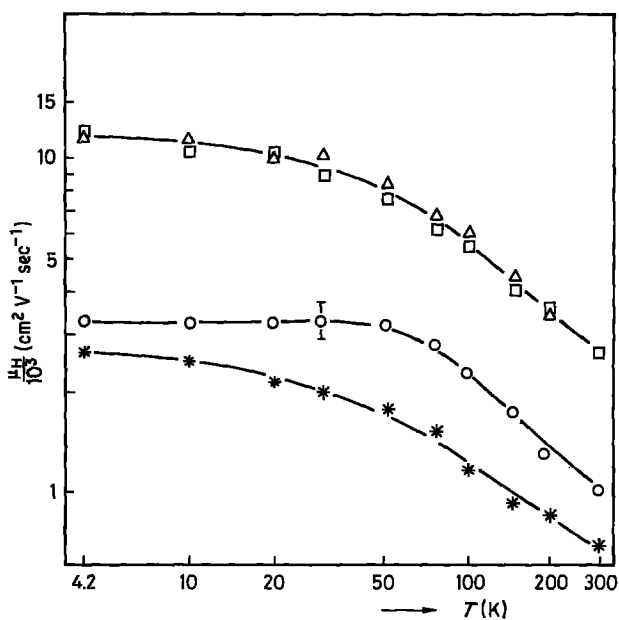


Figure 8 Mean Hall mobility μ_H of graphite/ AsF_5 compounds ($\text{C}_{8n}\text{AsF}_5$) plotted against temperature T for stage 1 (*), stage 2 (O), stage 3 (Δ) and stage 4 (\square). Error-bar is representative of all data points.

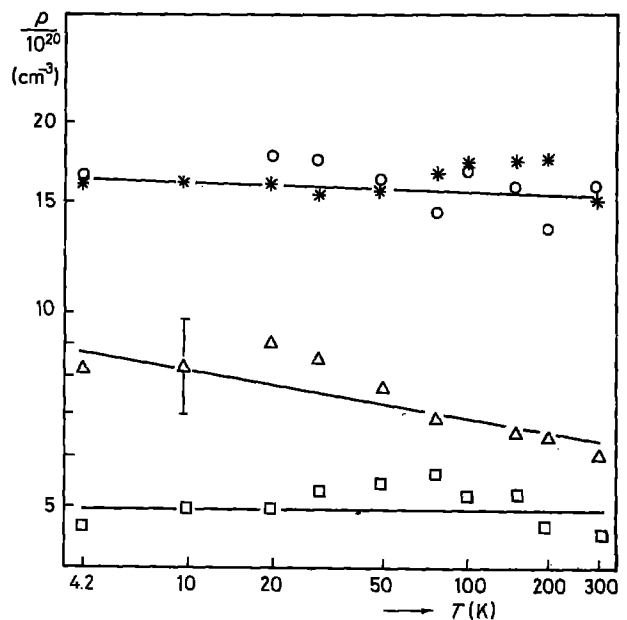


Figure 9 Total hole concentration p of graphite AsF_5 /compounds ($\text{C}_{8n}\text{AsF}_5$) plotted against temperature T for stage 1 (*), stage 2 (O), stage 3 (Δ) and stage 4 (\square). Error-bar is representative of all data points.

$\sigma_{ab}(4.2\text{ K})/\sigma_{ab}(300\text{ K}) \geq 15$, whereas the ratio for our graphite was between 2 and 3. Nevertheless the conductivity ratio of stage 1 $\text{AsF}_5/\text{graphite}$ varies from 6.8 to 14 [5] to 3.5 (present work). Using the rigid-band approximation, leaving the graphite band essentially unchanged by intercalation, it is clear that the sensitivity of transport properties of graphite to structural defects caused by nearly equal numbers of electrons and holes, is heavily reduced by a shift of the Fermi-level due to intercalation.

The two-dimensional band model of Blinowski and co-workers [23, 24] is based on the periodic structure of the intercalant sheets. This model uses the tight-binding approximation considering intra- and inter-layer nearest-neighbour interactions and neglecting dispersion along the stacking direction. As a result, valence and conduction bands are split into n sub-branches, where n is the stage index. A single band model is therefore only justified for stage 1 compounds. Since the evaluation of carrier properties in a multi-carrier model is not possible from the present set of data, and has not been satisfactory for stage 2 $\text{SbF}_5\text{-GICs}$ [25], galvanomagnetic data were analysed in terms of mean mobilities and total carrier concentrations. This simplification seems reasonable under the aspect that the mobility of the two hole types in a stage 2 acceptor-intercalated HOPG differ only by a factor of about 2 [25], so that light-carrier galvanomagnetic effects would not be expected.

The temperature dependence of the Hall mobility in graphite/ AsF_5 compounds is quite similar to that in HOPG determined from magnetoresistance [16]. For low temperatures defect scattering with a constant mean free path, l_b , is assumed to predominate. Scattering at grain boundaries and at the edges of Daumas-Herold domains limits l_b . The value of l_b was estimated from experimental data of the stage 1 compound:

$$l_b = \frac{m^* v_F \mu}{e} \quad (7)$$

where $m^* = 0.38m_0$ [7], is the effective mass, $v_F = 1.06 \times 10^8 \text{ cm sec}^{-1}$ [26] the Fermi velocity, and μ the drift mobility in the basal plane direction. For μ the value of the Hall mobility was used. The resulting diameter of defect-free domains is $0.6 \mu\text{m}$, which within experimental uncertainty equals the value obtained for HOPG [16]. The conclusion is drawn that the grain size in polycrystalline graphite is not reduced upon intercalation and no noticeable enhancement of defect concentration takes place. Furthermore it is concluded that either scattering at the edges of Daumas-Herold domains does not affect transport properties significantly, or that the size of the domains is at least equal to the dimensions of the microcrystallites.

Although one would expect a T^{-1} dependence of the Hall mobility in the high-temperature regime where phonon scattering predominates, $\mu_H \propto T^{-0.7}$ was observed, indicating contributions from other scattering mechanisms. The transition from the constant mobility at low temperatures which is due to defect scattering, to the high-temperature regime is more gradual than it is in HOPG [16]. In a calculation of Pietronero and Strässler [27] scattering at the

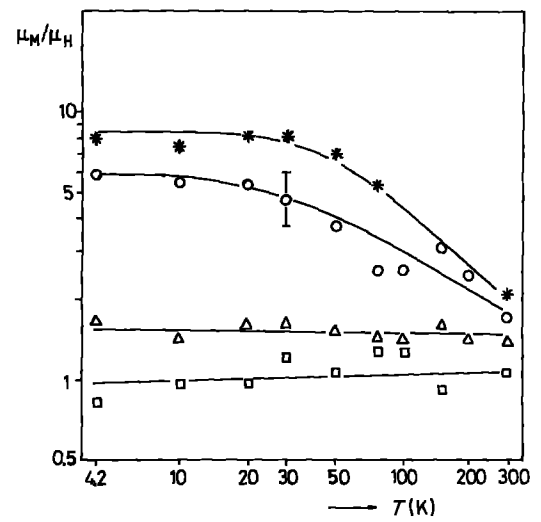


Figure 10 Ratio μ_M/μ_H of mobilities deduced from magnetoresistance (μ_M) and Hall effect (μ_H) measurements of graphite/ AsF_5 compounds ($\text{C}_{8n}\text{AsF}_5$), plotted against temperature T for stage 1 (*), stage 2 (O), stage 3 (Δ) and stage 4 (\square). Error bar is representative of all data points.

phonons of the charged intercalated molecules is found to be dominant between 20 and 100 K and washes out the kink in the mobility-temperature curve.

Although the band model of Blinowski and co-workers [23, 24] is consistent with conductivity and Hall effect measurements it cannot explain the magnetoresistance data. From the single-band dispersion relationship for stage 1 compounds only a small magnetoresistance is expected and saturation of $\Delta Q/Q_0$ for low magnetic fields where $\mu_M B \ll 1$ still holds, should not occur. In the stage 2 and higher-stage models, $\Delta Q/Q_0$ may be fitted to multicarrier magnetotransport theory, but yields no agreement with charge transfer values determined by other methods [25]. The divergence between magnetoresistance and Hall mobility is illustrated in Fig. 10 for stages 1 to 4 in the temperature range 4.2 to 300 K. For stages 2 to 4, μ_M and μ_H are mean mobilities deduced using Equations 3 and 4. The agreement of the two mobility values is satisfying for stage 3 and 4 compounds, considering the different scattering factors r_H and T_M respectively. With enhanced intercalation a strong increase in μ_M/μ_H is observed for low temperatures, reaching 8 for a stage 1 compound at 4.2 K. It should be noted, that the discrepancy is strongly reduced for temperatures where phonon scattering becomes predominant. This anomaly can be related to "trigonal warping", a deviation of the Fermi surface from cylindrical symmetry. That means, that the shape of the constant-energy surface has triangular symmetry when viewing in the stacking direction. Since trigonal warping is also important in the interpretation of low-field galvanomagnetic data of pristine graphite [28–30] consequences for magnetotransport in GICs are expected. Sugihara [31] estimated the contribution to low-field magnetoresistance to be one order larger than the classical effect in a stage 2 compound, and pointed out that the influence of trigonal warping on the Hall effect is far less pronounced. A calculation of Holz-

TABLE II Electrical charge transfer of graphite/AsF₅ intercalation compounds of different stages at room temperature determined by various experimental methods. (Values marked by * are taken at temperatures ranging from 1.2 to 4.2 K, but may be compared with room temperature results, since f is independent of temperature)

Method	Charge transfer f			
	$n = 1$	$n = 2$	$n = 3$	$n = 4$
Hall effect and conductivity (present work)	0.21–0.25	0.30–0.35	0.18–0.24	0.17–0.19
Magnetoresistance and conductivity [5]	0.15	–	–	–
Magnetic spin susceptibility [6]	0.24	0.48	–	–
Optical reflectivity [1]	0.41	0.53	–	–
Shubnikov–de Haas oscillations [7]	0.37*	0.41*	0.43*	–
De Haas–van Alphen oscillations [8]	–	0.22*	0.22*	0.26*
De Haas–van Alphen oscillations [9]	–	0.42*	–	–

worth [32] yields a saturation magnetoresistance of about 20% for a stage 1 compound at low temperatures even for weak magnetic fields where $\mu_M B \geq 0.3$. Following Sugihara the contribution of trigonal warping to magnetotransport becomes less important when the Fermi level is lowered in accordance with experimental data for higher stage compounds where $\mu_M/\mu_H \sim 1$ for stages $n = 3$ and 4 and no saturation of $\Delta\rho/\rho_0$ was observed for stage $n = 4$. From these results it seems reasonable to determine the mobility of acceptor-GICs via the Hall effect in order to avoid overestimations caused by trigonal warping.

Another effect observed in the magnetoresistance of low-stage compounds is the decrease of $\Delta\rho/\rho_0$ at high magnetic fields present only at low temperatures (see Fig. 7). Since this behaviour was not reported in previous work on AsF₅ and SbF₅-GICs [5, 25] it could very likely be related to the microcrystalline structure of the material. The shape of the curve can be fitted assuming a positive part of the magnetoresistance with saturation at higher fields, such as, for example, in the stage 3 sample at 4.2 K (Fig. 6) in competition with a negative part, becoming important at fields, where the saturation plateau is reached.

A possible mechanism for this negative $\Delta\rho/\rho_0$ was proposed by Fujita [33]. The mean free path of carriers is increased in a magnetic field due to a deflection from the straight-forward motion and to diffuse scattering at crystallite boundaries. The reduction of resistivity is proportional to B^2 provided that the diameter of the circular carrier motion is greater than the crystallite dimensions, and boundary scattering is the dominant mechanism, e.g. at low temperatures where no phonon scattering is present. From Fig. 7 it is seen that the negative magnetoresistance effect is washed out with increasing temperature due to phonon scattering. The diameter, d , of the circular hole path may be estimated, using m^* and v_F values of a stage 1 compound given above, to yield

$$d = (2m^*v_F)/(eB) \quad (8)$$

At $B = 10$ kG the path diameter is $4.6 \mu\text{m}$ which is much greater than the mean crystallite dimensions ($0.6 \mu\text{m}$). For stages 3 and 4 where the magnetoresist-

ance reduction was not observed, the diameter of the hole path is distinctly smaller as a consequence of lower effective masses (Equation 8) and the prerequisites for negative magnetoresistance according to this model are no longer valid. A similar effect may occur with high-grade HOPG where crystallite size is up to $40 \mu\text{m}$ diameter [34]. For a further test of this model, magnetoresistance data for magnetic fields greater than 10 kG would be needed.

The charge transfer, f , is one of the main parameters for the description of GICs since it determines the Fermi level and the carrier concentration. On the other hand, a chemical charge transfer f_{chem} is defined by the reaction equilibrium of the disproportioning reaction Equation 5. Assuming that the electron uptake on the left side of Equation 5 is the main reason for the hole generation in the highly conducting graphite layers, electrical and chemical charge transfer are equivalent and the hole concentration equals in a first approximation the concentration of AsF₆⁻ ions. There has been a lot of controversy whether Reaction 5 goes completely to the right side, yielding $f_{\text{chem}} = 2/3$ or not [21, 35, 36].

From the present results of Hall effect and electrical conductivity, f is determined and compared with conclusions from other experiments in Table II. In contrast to donor-GICs, where f is approximately equal to unity [37], the charge transfer of graphite/AsF₅ is distinctly lower. In agreement with all measurements, the maximum value $f = 2/3$ is not reached, which means that only about half of the AsF₅ molecules disproportionate during intercalation. Charge transfer does not change with temperature in the range from 4.2 to 300 K, but is dependent on the intercalation stage. All measurements agree in an enhancement of f from stage 1 to stage 2, which may be due to electrostatic shielding of the neighbouring intercalation layer by the second graphite sheet. This would raise expectations for a further increase of f for higher-stage compounds as observed by quantum oscillatory effects [7, 8], whilst our results indicate a decrease of charge transfer. Since f would be affected by the degree of ordering of intercalated molecules, a detailed model for higher stage compounds would be necessary.

5. Conclusions

In this paper a study of the transport properties of all stages of AsF_5 -graphite intercalation compounds in the temperature range from 4.2 to 300 K is reported. Contactless eddy current methods for conductivity and magnetoresistance measurements and a new inductive technique for the Hall effect have been applied. Electrical in-plane conductivity at room temperature reaches about half the value of copper for a stage 2 compound. The temperature dependence of the conductivity follows a T^{-1} law at higher temperatures with kinks at 140 and 130 K for stage 1 and stage 2 samples, respectively, indicating an electronic transformation in the intercalant layers. P-type conduction was found, in agreement with the strong electronegativity of AsF_5 . From the temperature dependence of the hole mobility, scattering at crystallite boundaries at low temperatures, at phonons of the intercalated molecules between 20 and 100 K, and at graphite phonons above 100 K is deduced. For the higher-temperature region, a $T^{-0.7}$ rather than a T^{-1} dependence was found. This may be considered as an indication for additional scattering mechanisms. The mobility of HOPG is degraded by an order of magnitude upon intercalation, which is mainly due to an effective-mass increase caused by the Fermi-level shift and not due to additional defects in the material. Therefore the observed conductivity data are believed to be already intrinsic properties and may not be considerably enhanced by more refined synthesizing techniques. The magnetoresistance of low-stage compounds shows strong anomalies at low temperatures, which may lead to an overestimation of the carrier mobility. Enhanced magnetoresistance for low magnetic fields and saturation in a field range, where $\mu_M B < 1$, may be due to trigonal warping of the energy bands in the layer plane. In addition, a negative magnetoresistance component was observed in stage 1 and 2 compounds at low temperatures. The effect is interpreted by diffuse carrier scattering at crystallite boundaries. It is not observed if phonon scattering becomes predominant. The charge transfer, determined by conductivity and Hall effect measurements, is found to be temperature independent, reaching a maximum value of 1/3 for stage 2 compounds. This indicates that about half of the intercalated AsF_5 molecules are left unaffected between the graphite layers.

Acknowledgements

We are grateful to Professor Ian L. Spain for the donation of HOPG samples. The work was supported by Stiftung Volkswagenwerk, FRG, and the Fonds zur Förderung der wissenschaftlichen Forschung, Austria.

References

1. M. SAINT JEAN, NGUYEN HY HAU and C. RIGAUX, *Solid State Commun.* **46** (1983) 55.
2. G. M. T. FOLEY, C. ZELLER, E. R. FALARDEAU and F. L. VOGEL, *ibid.* **24** (1977) 371.
3. L. V. INTERRANTE, R. S. MARKIEWICZ and D. W. McKEE, *Synth. Met.* **1** (1979/80) 287.

4. T. E. THOMPSON, E. M. McCARRON and N. BARTLETT, *ibid.* **3** (1981) 255.
5. C. ZELLER, L. A. PENDRYS and F. L. VOGEL, *J. Mater. Sci.* **14** (1979) 2241.
6. B. R. WEINBERGER, J. KAUFER, A. J. HEEGER, J. E. FISCHER, M. MORAN and N. A. HOLZWARTH, *Phys. Rev. Lett.* **41** (1978) 1417.
7. R. S. MARKIEWICZ, H. R. HART Jr, L. V. INTERRANTE and J. S. KASPER, *Synth. Met.* **2** (1980) 331.
8. S. TANUMA, Y. IYE, O. TAKAHASHI and Y. KOIKE, *ibid.* **2** (1980) 341.
9. J. E. FISCHER, M. J. MORAN and J. W. MILLIKEN, *Solid State Commun.* **39** (1981) 439.
10. E. R. FALARDEAU, L. R. HANLON and T. E. THOMPSON, *Inorg. Chem.* **17** (1978) 301.
11. J. G. HOOLEY, *Mater. Sci. Eng.* **31** (1977) 17.
12. H. E. RORSCHACH and M. A. HERLIN, Massachusetts Institute of Technology, Technical Report no. 125 (1952).
13. C. ZELLER, G. M. T. FOLEY, E. R. FALARDEAU and F. L. VOGEL, *Mater. Sci. Eng.* **31** (1977) 255.
14. M. E. POTTER, W. D. JOHNSON and J. E. FISCHER, *Solid State Commun.* **37** (1981) 713.
15. W. LANG, A. PHILIPP and K. SEEGER, to be published.
16. *Idem*, to be published.
17. I. L. SPAIN and D. J. NAGEL, *Mater. Sci. Eng.* **31** (1977) 183.
18. M. S. DRESSELHAUS and S. Y. LEUNG, Extended Abstracts of 14th Biennial Conference on Carbon, Pennsylvania State University (American Carbon Society, 1979) p. 496.
19. B. R. WEINBERGER, J. KAUFER, A. J. HEEGER, E. R. FALARDEAU and J. E. FISCHER, *Solid State Commun.* **27** (1978) 163.
20. S. K. KHANNA, E. R. FALARDEAU, A. J. HEEGER and J. E. FISCHER, *ibid.* **25** (1978) 1059.
21. N. BARTLETT, R. N. BIAGIONI, B. W. McQUILLAN, A. S. ROBERTSON and A. C. THOMPSON, *J. Chem. Soc. Chem. Commun.* (1978) 200.
22. I. L. SPAIN, *Chem. Phys. Carbon* **8** (1973) 1.
23. J. BLINOWSKI, NGUYEN HY HAU, C. RIGAUX, J. P. VIEREN, R. LETOULLEC, G. FURDIN, A. HEROLD and J. MELIN, *J. Phys.* **41** (1980) 47.
24. J. BLINOWSKI and C. RIGAUX, *ibid.* **24** (1980) 667.
25. I. L. SPAIN and K. J. VOLIN, *Mater. Res. Soc. Symp. Proc.* **20** (1983) 173.
26. L. PIETRONERO, S. STRÄSSLER and H. R. ZELLER, *Solid State Commun.* **30** (1979) 399.
27. L. PIETRONERO and S. STRÄSSLER, *Synth. Met.* **3** (1980) 213.
28. R. O. DILLON and I. L. SPAIN, *J. Phys. Chem. Solids* **39** (1978) 923.
29. H. OSHIMA, K. KAWAMURA, T. TSUZUKU and K. SUGIHARA, *J. Phys. Soc. Jpn.* **51** (1982) 1476.
30. K. SUGIHARA, S. ONO, H. OSHIMA, K. KAWAMURA and T. TSUZUKU, *ibid.* **51** (1982) 1900.
31. K. SUGIHARA, *Mater. Res. Soc. Symp. Proc.* **20** (1983) 179.
32. N. A. W. HOLZWARTH, *Phys. Rev. B.* **21** (1980) 3665.
33. F. FUJITA, *Carbon* **6** (1968) 746.
34. A. W. MOORE, *Chem. Phys. Carbon* **11** (1973) 69.
35. L. B. EBERT, D. R. MILLS and J. C. SCANLON, *Mater. Res. Bull.* **14** (1979) 1369.
36. M. J. MORAN, J. E. FISCHER and W. R. SALANECK, *J. Chem. Phys.* **73** (1980) 629.
37. D. GUÉRARD, G. M. T. FOLEY, M. ZANINI and J. E. FISCHER, *Il Nuovo Cimento* **38B** (1977) 410.

Received 2 January
and accepted 6 May 1986